Natural Hazards
https://doi.org/10.1007/s11069-022-05279-x

ORIGINAL PAPER

Anthropogenic sinkholes of the city of Naples, Italy: an update

Rita Tufano[1] · Luigi Guerriero[1] · Mariagiulia Annibali Corona[1] · Giuseppe Bausilio[1] · Diego Di Martire[1] · Stefania Nisio[2] · Domenico Calcaterra[1]

Received: 13 August 2021 / Accepted: 10 February 2022

Abstract
In recent years, the study of anthropogenic sinkholes in densely urbanized areas has attracted the attention of both researchers and land management entities. The city of Naples (Italy) has been frequently affected by processes generating such landforms in the last decades: for this reason, an update of the sinkhole inventory and a preliminary susceptibility estimation are proposed in this work. Starting from previous data, not modified since 2010, a total of 270 new events occurred in the period February 2010–June 2021 were collected through the examination of online newspapers, local daily reports, council chronicle news and field surveys. The final consistence of the updated inventory is of 458 events occurred between 1880 and 2021, distributed through time with an increasing trend in frequency. Spatial analysis of sinkholes indicates a concentration in the central sector of the city, corresponding to its ancient and historic centre, crossed by a dense network of underground tunnels and cavities. Cavity-roof collapse is confirmed as one of the potential genetic types, along with processes related to rainfall events and service lines damage. A clear correlation between monthly rainfall and the number of triggered sinkholes was identified. Finally, a preliminary sinkhole susceptibility assessment, carried out by Frequency Ratio method, confirms the central sector of city as that most susceptible to sinkholes and emphasizes the predisposing role of service lines, mostly in the outermost areas of the city.

Keywords Anthropogenic sinkholes · Inventory · Cavities · Triggering factors · Collapse sinkholes

1 Introduction

Sinkholes are widespread in many regions of the world, such as Florida, China, Ecuador, Iran, Turkey (Wilson and Beck 1992; Jiang et al. 2005; Lei et al. 2005; Brinkmann et al. 2008; Karimi and Taheri 2010; Heidari et al. 2011; Gao et al. 2013; Ozdemir 2015, 2016;

✉ Luigi Guerriero
luigi.guerriero2@unina.it

[1] Department of Earth, Environmental and Resource Sciences, Federico II University of Naples, 80126 Naples, Italy

[2] ISPRA, Institute for Environmental Protection and Research, Rome, Italy

Taheri et al. 2015; Kim et al. 2017; Subedi et al. 2019; Cando Jàcome et al. 2020) and represent a relevant geohazard due to their frequent and sudden development (Newton 1984; Sinclair and Steward 1985; Beck and Jenkins 1986; Snyder et al. 1989; Nisio et al. 2007). The term sinkhole is used to indicate a subcircular depression/collapse which occurs in a range of geological conditions. For instance, in karst environment such landforms develop due to subsurface chemical dissolution of rocks (solution sinkholes) or by both subsurface dissolution and downward gravitational movement (internal erosion or deformation) of the undermined overlying material (subsidence sinkholes) (Waltham et al. 2005; Gutiérrez et al. 2008, 2014); in alluvial plains characterized by thick deposits of alluvium, or intercalations of volcaniclastic products, colluvial deposits and clays, sinkholes originate from soil piping and related voids collapse (Parise and Gunn 2007; Del Prete et al. 2010; Iovine et al. 2016).

In the presence of natural or man-made underground cavities, instabilities related to roof failure into underlying cavities are responsible for generating collapse sinkholes (Ammirati et al. 2020). Their origin is linked to variations of stress conditions that exceed material strength in the surroundings, frequently related to sudden water-level changes (Tharp 1999, 2002; Shalev and Lyakhovsky 2012) or to the degradation of the rock mass, due to water infiltration, weathering processes, etc.… (Parise 2015). This failure mechanism, although frequently associated to soluble rocks, is also typical in soft rocks as tuffs, loess and sandstones, characterized by the presence of cavities. The general formation of this type of sinkholes consists in the initial collapse at the roof of the cavity, that can propagate to the ground surface as a function of the cavity geometry and of the physical, mechanical and hydraulic properties of the materials (Scotto di Santolo et al. 2018).

Underground cavities can be a common element in urban areas, especially in the presence of bedrock materials suitable for settlement built up and can have significant effects on sinkhole development due to their predisposing action. Worldwide, several case studies of the collapse of man-made underground cavities in urban areas have been proposed, as for example the study case of the two systems of bell-shaped chalk caverns in Israel (Hatzor et al. 2002), the abandoned metal mines in Canada (Bètournay 2009), some limestone mines in the Netherlands (Bekendam 1998) and the Longyou rock caverns in China (Li et al. 2009). In urban areas, sinkhole initiation may be responsible for severe damage to settlements and in some cases for the loss of human life, so that they can be considered as an emerging hazard of the Anthropocene (Dixon et al. 2018). In this context, the analysis of sinkholes susceptibility and hazard has significant implications for human society and should guide urban planning and emergency plan development.

Over the last decades, the occurrence of sinkholes in urban areas has substantially increased (Pellicani et al. 2017). In Italy sinkholes are widespread, with over 50% of them located in the central-southern regions (Nisio et al. 2007; Parise and Vennari 2013). Of these, sinkholes caused by the roof failure of man-made cavities (or anthropogenic sinkholes) have been recognized in Apulia (Parise 2011; Parise and Lollino 2011; Lollino et al. 2013; Fazio et al. 2017; Pellicani et al. 2017), Sicilia (Sottile 2016) and in Campania region (Guarino and Nisio 2012; Scotto di Santolo et al. 2015, 2016, 2018; Cennamo et al. 2017; Guarino et al. 2018; Rispoli et al. 2020). In this context, the risk linked to anthropogenic sinkholes is relevant for the communities, also in relation to their very rapid development that may prevent any tentative to escape. In these cases, an important tool for risk mitigation is the development of susceptibility and hazard scenarios, based on updated inventories, that provide information on the distribution of existing sinkholes in a given area. Sinkhole inventories are of fundamental importance for draft susceptibility maps and for the selection and application of mitigation measures and adaptation plans

(Waltham et al. 2005; Gutièrrez et al. 2008, 2014). Sinkhole susceptibility maps can be produced through several methods with different abilities and predictive accuracy, including probabilistic (Kim et al. 2006; Galve et al. 2009), multicriteria decision (Mancini et al. 2009), artificial neural network (ANN) (Kim et al. 2009), and fuzzy operator (Choi et al. 2010) analyses. Among the probabilistic methods, Frequency Ratio is widely used to perform sinkhole susceptibility mapping (i.e. Yilmaz 2007; Oh and Lee 2011; Pradhan et al. 2014). Frequency Ratio is defined as the ratio of the probabilities of a sinkhole occurrence to a non-occurrence for a given attribute, used to obtain relationships between predisposing factors chosen and sinkhole occurrence area.

Anthropogenic sinkholes, due to their spatial and temporal distribution, are among the most relevant issues in the densely urbanized municipality of Naples (over 8,000 inhabitants/km^2 in 2019—ISTAT 2019). For instance, the ancient center of the city (dating back to seventh century B.C.), worldwide known for cultural heritage expression of its long history, is particularly prone to collapse sinkholes due to the presence of a network of underground cavities, the oldest of which refer to the Eneolithic age (Fig. 1) (Basso et al. 2013). According to the international classification of artificial cavities (Galeazzi 2013; Parise et al. 2013), the most common categories present in the subsoil of the city of Naples can be identified, with respect to the building techniques, as: (1) cavities dug in the subsoil and (2) cavities constructed in the subsoil. Instead, the type of underground artificial structures can be recognized as: (1) aqueducts, cisterns and sewer systems (type A.3, A.4 and A.7); (2) hypogeum (type B.1); (3) cultural places (type C.1); (4) cavities derived from quarrying of bedrock tuff material (as building material) (type E.1). All such artificial cavities are today sites of preferential weathering of the rock mass, suffering a slow but continuous decay that creates predisposing conditions for sinkhole development. Many cavities are currently abandoned, neglected and/or inaccessible because filled with buildings debris or other

Fig. 1 Photos of man-made underground cavities of the city of Naples: **a** *Cimitero delle Fontanelle* (courtesy of Sintema Engineering srl); **b**, **c** *San Marcellino* cavity

materials (Evangelista et al. 2000), so that it is challenging to know their precise planimetric and volumetric extension. In some cases, places of worship, such as architectural elements, are located just in correspondence of cavities, making them potentially susceptible to damage related to cavity-roof collapse sinkholes (Rispoli et al. 2020).

In the perspective of an estimation of sinkhole risk, this paper presents an update of sinkhole inventory and a preliminary susceptibility assessment for the city of Naples. Starting from the dataset produced by Guarino and Nisio (2012), consisting of 188 anthropogenic sinkholes occurred between 1880 and 2010, a new inventory was prepared adding the events occurred between February 2010 and the first half of 2021. The information related to sinkhole occurrence was derived from different sources, including newspapers to field survey, and an analysis of the genesis mechanisms and of the triggering factors, responsible for sinkholes formation, was also carried out. Subsequently, a preliminary sinkhole susceptibility assessment was developed through the Frequency Ratio analysis (Bonham-Carter 1994), based on the statistical relationships between the total inventory of sinkholes and 12 predisposing factors.

2 The study area

The city of Naples (Fig. 2) lies in the Campanian Plain, an asymmetric half-graben (D'Argenio et al. 1973; Brancaccio et al. 1991; Milia et al. 2003; Turco et al. 2006; Vitale and Ciarcia 2018) filled by a 2000–3000-m-thick sequence of Quaternary continental, deltaic, marine sediments and volcanic deposits derived from the activity of Phlegraean Fields district and Somma-Vesuvius volcano. The hilly morphology of the area surrounding

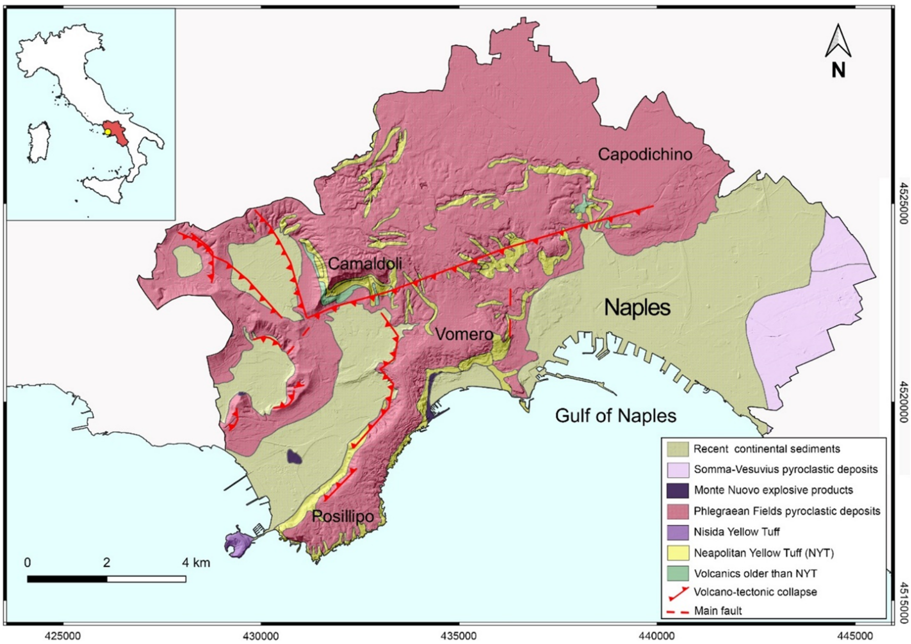

Fig. 2 Geological map of the city of Naples

the city is consistently related to the activity of explosive monogenetic volcanoes of the Phlegraean Fields as well as to volcanic-tectonic collapses linked to the formation of the Campanian Ignimbrite — CI (39 ky) and of Neapolitan Yellow Tuff — NYT (15 ky) caldera (Scarpati et al. 2013). NYT forms the urban bedrock and consists mostly of pyroclastic-flow and minor fall deposits that can be ascribed either to lithified or not-lithified diagenetic facies. The former has a yellow colour, while the latter, the so-called Pozzolana, is grey and preserves its primary depositional character. In particular, lithification is the result of a diagenetic zeolitisation process (Scarpati et al. 1993).

The NYT eruption is among the most relevant of the history of the Phlegraean Fields. After this eruption, about 70 episodes occurred over three epochs of activity (15.0–9.5, 8.6–8.2 and 4.8–3.8 ky) with a mean recurrence interval of a few tens of years (Orsi et al. 2004). Such eruptions produced loose pyroclastic deposits, pyroclastic flows and surge deposits, mainly observable in the western sector of the city. In this area, several meters of such pyroclastic deposits cover NYT, appearing particularly thick (up to 30 m) at the base of hillslopes where they fill structural depressions or ancient erosional valleys (Cinque et al. 2011). Instead, in the central sector of the city NYT is unconformably followed upward by a sequence (usually 15 m thick) alternating reworked and in situ pyroclastics carrying at the base the fallout deposits of the Soccavo eruption (10.3–9.5 ka; Amato et al. 2009). In the eastern zone of the city, alluvial sediments and marshes fill the Sebeto River alluvial plain, developed in the tectonic depression of Volla (Bellucci et al. 1993). In the urban coastal plains and in the northern and western sectors of the city, marine to continental sediments are also present, usually covered by landfills.

The landscape of Naples is also characterized by incision activities from superimposed torrents, alternating small coastal bays (sometimes hosting narrow coastal plains) and cliffed promontories (Cinque et al. 2011). From a hydrogeological point of view, the Neapolitan subsoil is marked by an unconfined aquifer housed in the pyroclastic rocks overlying the NYT. The water table is generally located at variable depths below the surface, ranging from 20 m to more than 200 m, except for the morphologically depressed areas, such as in the Sebeto River plain and the areas near the coast, where it is close to the ground surface (Guarino and Nisio 2012).

A singular feature of the city is the presence of an extended network of underground cavities of variable shape, extent and volume, located within the NYT. For its peculiar characteristics as macro-porosity, fair mechanical parameters and low specific weight, this material has been intensely quarried and used as building stone in Neapolitan and regional architecture since Greek times. For many centuries, the extraction activity has been concentrated beneath the city of Naples. Subsequently, open pit quarries developed at the borders of the old town and more recently along the western sector of Campi Flegrei (Morra et al. 2010). Over the centuries, the network of underground cavities has grown also for the building of crypts, catacombs and cemeteries as well as aqueduct system and cisterns and subway lines (Evangelista et al. 2000; Scotto di Santolo et al. 2015; Allocca et al. 2018). In many cases, their exact location is unknown.

3 Materials and methods

As a first step toward the development of an updated inventory of anthropogenic sinkholes of the city of Naples, data and information related to sinkhole phenomena documented by ISPRA (*Italian National Institute for Environmental Protection and Research*) inventory

(Guarino and Nisio 2012) were digitalized in vector format within a Geographic Information System (GIS). Subsequently, sinkholes occurred between February 2010 and June 2021 were added to the inventory. Information about such events were derived from multiple sources: (1) online version of national daily newspapers (e.g. www.ansa.it, www.corriere.it, www.ilmattino.it), (2) local daily reports (e.g. www.fanpage.it/napoli/, www.napolitoday.it, www.vesuviolive.it), (3) council chronicles news (e.g. from www.comune.napoli.it) and (4) field survey carried out by the authors. For each inventoried event, data relative to sinkhole occurrence were verified by cross-correlating different sources. In this way, the risk of introducing inconsistent information was reduced.

For each new event collected, data about formation timing (generally day, month and year), location (in terms of WGS84-UTM coordinates or, when not possible, of indication of the street of occurrence), sources, presumable triggering factor, were derived from newspaper information and field evidence (for those collected by field survey; e.g. the evident rupture of an aqueduct line). Main morphometric characteristics (diameter and depth) and a photo of the event were derived whenever possible, too. Moreover, interviews to locals were conducted to obtain specific information on sinkholes. Some information, as the exact location and the morphometric characteristics of sinkholes, were not always available or well indicated. In these cases, it was necessary to conduct a visual inspection of the available photos and an additional spatial analysis into Google Earth environment, to identify the location and assess the diameter of the sinkhole. Figure 3 shows a few examples of photographic documentation used for the event recognition. To supplement our analysis, providing an interpretation of the sinkhole-driving mechanism, data depicting the presence and distribution of the cavities over the study area and rainfall data derived from Napoli Capodimonte station (#18949) for the period 2010–June 2021, were acquired. In this way, connections between anthropogenic triggering factors and/or rainfall events leading to sinkhole occurrence in the study area were investigated through graphical correlations.

Preliminary sinkhole susceptibility assessment was carried out using the dataset of events for which coordinates of occurrence are known, through the Frequency Ratio model

Fig. 3 Examples of sinkholes located in the city of Naples: **a** Via Girolamo Santacroce, Vomero municipality, 15/02/2019; **b** viale Calascione a Monte di Dio, 08/11/2019; **c** via Jacopo De Gennaro, Fuorigrotta municipality, 18/12/2019 (modified from www.ilmattino.it); **d** parking of Ospedale del Mare, 08/01/2021

(Bonham-Carter 1994), and considering twelve predisposing factors *PFs* (1—Aqueduct Network Density; 2- Aqueduct Network Distance; 3—Groundwater depth; 4—Cover thickness; 5—Road Network Density; 6—Road Network Distance; 7—Sewer System Density; 8—Sewer System Distance; 9—Underground Cavity Density; 10—Underground Cavity Distance; 11—Underground Railroad Density; 12—Underground Railroad Distance). This approach allows the calculation of the probability of appearance of new phenomena considering five different classes of decreasing weight for each predisposing factor and on the base of already known sinkholes data occurrence. Frequency Ratio (*FR*) was estimated through the formulation (1):

$$\mathrm{FR}_{\mathrm{score}} = \frac{\text{Number of pixels with sinkholes for the class of PF} / \text{Total number of pixels with sinkholes}}{\text{Number of pixels of the class of PF/Total number of pixels}} \tag{1}$$

with a pixel size of 20×20 m. After calculating FR score for each class of predisposing factors, a Sinkhole Susceptibility index was calculated by the sum of the FR scores. The result was reclassified in five different susceptibility classes from very low to very high using the Natural Breaks classification method (Jenks 1967). Finally, performance of the model was determined by the Area Under the Curve (AUC) of the relative Receiver Operating Characteristics (ROC) curve (Swets 1988).

4 Results

4.1 The updated inventory

Sinkhole recognition through online newspapers, local daily reports, council chronicle news, literature analysis (i.e. existing ISPRA database—Guarino and Nisio 2012) and field surveys, was carried out producing an inventory of 458 anthropogenic sinkholes of the city of Naples, 270 of which triggered between February 2010 and June 2021 (Table 1). Of the 458 inventoried sinkholes, 455 bear associated information about time of occurrence. The yearly frequency of sinkholes since the second half of the last century (data prior than 1950 have been represented as a single data value) highlights the enrichment of inventory with the most recent data (Fig. 4a). The entire series is characterized by a general increasing trend, although the distribution is quite discontinuous. In fact, some periods prior to the update are characterized by an absence of events, probably due to a non-significance of news, or to a possible loss of information. However, since 2007 and until June 2021, about 61% of the 455 inventoried sinkholes (known timing of occurrence) form a continuous series sharply growing with time. Such percentage is formed by 13 events from ISPRA inventory and 267 sinkholes occurred between February 2010 and June 2021. Sinkholes from ISPRA inventory are 188, while the new inventoried events are 270, 267 of which with of known timing of occurrence (Fig. 4a).

Overall, inventoried sinkholes were triggered by: rainfall events, aqueduct and sewer leaks and maintenance works; however, in 36.0% of the cases, triggering factors were not identified. The comparison between triggering factors (Fig. 4b) shows for sinkholes inventoried by ISPRA that rainfall is recognized as the most common defined cause (50.5% of the events), followed by not defined factors (22.9%), aqueduct and sewer leaks (9.6%) and maintenance works (2.1%); while for February 2010–June 2021 sinkholes the most common factor is not defined (45.2% of events), followed by rainfall (37.0%), aqueduct and sewer leaks (15.6%) and maintenance works (2.2%).

Table 1 Sinkholes occurred in the period 2010–June 2021 in Naples

N	Date	WGS84—UTM-E	WGS84—UTM-N	Location	Factor	Diameter (m)	Depth (m)
1	n.d	4,526,737	437,838	Via Monte Grappa, 87	R	n.d	n.d
2	n.d	4,526,635	436,431	Via Teano, 34/38	A	n.d	n.d
3	n.d	4,526,602	436,486	Via Teano, 14/18	A	n.d	n.d
4	10/02/2010	4,520,767	436,357	Piazza Santa Maria degli Angeli	T	n.d	n.d
5	18/02/2010	4,521,571	435,231	Via Domenico Cimarosa, 65	S	1	1
6	19/02/2010	n.d	n.d	Via Leopardi	n.d	n.d	n.d
7	20/02/2010	4,521,243	436,867	Piazza Municipio	n.d	n.d	n.d
8	///10/2010	4,520,746	433,465	Via Torre Cervati	n.d	n.d	n.d
9	24/03/2010	4,521,548	436,979	Via Medina	n.d	n.d	n.d
10	14/04/2010	4,522,787	435,080	Piazza Muzii	T	n.d	n.d
11	14/05/2010	4,521,569	435,018	Via Cimarosa	R	n.d	n.d
12	29/06/2010	4,520,386	434,547	Largo Torretta	R	n.d	n.d
13	02/10/2010	4,525,558	435,068	Via Marco Rocco di Torrepadula	S	n.d	n.d
14	12/10/2010	4,522,046	434,898	Via Luca Giordano	n.d	n.d	n.d
15	10/11/2010	n.d	n.d	Viale Umberto Maddalena	n.d	n.d	n.d
16	18/12/2010	4,522,880	440,027	Via Emanuele Gianturco	n.d	n.d	n.d
17	24/12/2010	4,527,616	433,700	Via Santa Maria a Cubito	n.d	3	10
18	17/01/2011	n.d	n.d	Via Garibaldi	S	4	5
19	11/02/2011	4,522,198	434,470	Via Bruno Falcomatà	n.d	2	0.5
20	11/02/2011	4,522,203	434,462	Via Bruno Falcomatà	n.d	2	0.5
21	27/02/2011	4,521,066	431,792	Via Marco Aurelio, 155	n.d	n.d	n.d
22	27/02/2011	n.d	n.d	Vico Duchesca	n.d	n.d	n.d
23	28/04/2011	n.d	n.d	Piazza degli Artisti	n.d	n.d	n.d
24	24/09/2011	4,521,943	429,330	Via Sartania, 55	A	n.d	n.d
25	05/10/2011	n.d	n.d	Via Pizzone	n.d	n.d	n.d
26	21/10/2011	n.d	n.d	Via Bartolo Longo	n.d	n.d	n.d
27	26/10/2011	4,522,084	435,133	Via V. D'annibale	R	n.d	0.8

Table 1 (continued)

N	Date	WGS84—UTM-E	WGS84—UTM-N	Location	Factor	Diameter (m)	Depth (m)
28	01/11/2011	4,521,941	438,413	Via Amerigo Vespucci	n.d	n.d	n.d
29	06/11/2011	4,516,989	431,465	Via Tito Lucrezio Caro, 6	n.d	3	5
30	07/11/2011	4,523,234	438,308	Vico S. Maria della Fede, 2	R	3	0.5
31	08/11/2011	n.d	n.d	Via Ferrovia	n.d	n.d	n.d
32	08/11/2011	n.d	n.d	Via Sant'Ignazio di Loyola	n.d	n.d	n.d
33	08/11/2011	n.d	n.d	Via Consalvo	n.d	n.d	n.d
34	08/11/2011	4,522,991	435,046	Via Domenico Fontana, 49	n.d	3	0.5
35	28/11/2011	4,522,342	437,055	Piazza Miraglia	T	> 10	n.d
36	///11/2011	4,523,079	435,420	Vi a Carlo Cattaneo, 21	A	1.5	n.d
37	07/12/2011	4,522,321	430,882	Rotonda Don Giustino	n.d	n.d	n.d
38	04/02/2012	4,522,116	434,942	Via Luca Giordano	R	n.d	n.d
39	16/02/2012	4,521,583	436,631	Via Concezione a Montecalvario	n.d	n.d	n.d
40	16/02/2012	4,521,618	436,635	Via Lungo del Gelso, 114	n.d	1.5	1.5
41	17/03/2012	n.d	n.d	Via Vernicchi	n.d	2	2
42	26/03/2012	4,522,191	434,477	Via Bruno Falcomatà, 44	A	4	n.d
43	15/04/2012	n.d	n.d	Via Pigna	n.d	n.d	n.d
44	17/04/2012	n.d	n.d	Via Canale Olivella	R	n.d	n.d
45	17/04/2012	n.d	n.d	Via Broggia	R	n.d	n.d
46	17/04/2012	4,525,948	441,409	Via Cupa Arcamone	R	n.d	n.d
47	02/05/2012	n.d	n.d	Chiesa dei Santi Marcellino e Festo	n.d	n.d	n.d
48	17/05/2012	n.d	n.d	Via Giotto	n.d	n.d	n.d
49	06/06/2012	n.d	n.d	Via Lepanto	n.d	n.d	n.d
50	15/07/2012	4,516,925	430,993	Viale Virgilio	n.d	n.d	n.d
51	31/07/2012	4,521,848	434,781	Via Gino Doria, 102–106	A	n.d	n.d
52	06/08/2012	n.d	n.d	Via Tito Lucrezio Caro	n.d	n.d	n.d

Table 1 (continued)

N	Date	WGS84—UTM-E	WGS84—UTM-N	Location	Factor	Diameter (m)	Depth (m)
53	07/09/2012	n.d	n.d	Piazza Sannazzaro	n.d	3	1
54	23/10/2012	n.d	n.d	Via Vico Pacelle	n.d	n.d	n.d
55	31/10/2012	n.d	n.d	Via Pigna	n.d	n.d	n.d
56	09/11/2012	n.d	n.d	Via Fratelli Wright	n.d	n.d	n.d
57	01/12/2012	n.d	n.d	Via Leopardi	n.d	n.d	n.d
58	02/12/2012	4,522,471	436,791	Via Enrico Pessina	A	n.d	n.d
59	02/12/2012	4,526,365	437,058	Via della Liguria	R	4	2
60	10/01/2013	4,521,262	435,281	Via Filippo Palizzi	n.d	n.d	n.d
61	16/01/2013	4,524,237	436,602	Via Capodimonte	R	n.d	n.d
62	16/01/2013	4,524,093	436,504	Via Capodimonte, 16	R	n.d	n.d
63	16/01/2013	4,522,859	436,898	Piazzetta Gagliardi	R	n.d	n.d
64	15/02/2013	4,522,499	438,647	Corso Arnaldo Lucci	n.d	n.d	n.d
65	17/02/2013	4,520,940	435,506	Via Vittoria Colonna	n.d	n.d	n.d
66	08/03/2013	4,521,568	434,675	Via Belvedere	T	0.5	n.d
67	17/03/2013	4,521,464	437,375	Via Cristoforo Colombo	n.d	n.d	n.d
68	28/04/2013	4,520,919	436,618	Via Chiaia, 264–265	n.d	n.d	n.d
69	04/05/2013	n.d	n.d	Giardini di Poggio Reale	n.d	n.d	n.d
70	07/05/2013	4,520,492	436,143	Via Arcoleo	R	n.d	n.d
71	19/07/2013	4,524,249	433,897	Via Leonardo Bianchi, 27	S	n.d	n.d
72	08/10/2013	4,521,359	435,837	Gradoni Santa Maria Apparente, 10	S	1.8	1
73	25/11/2013	4,522,707	438,304	Corso Garibaldi	R	0.5	0.5
74	30/11/2013	4,522,498	436,794	Via Pessina	R	n.d	n.d
75	20/01/2014	4,524,611	438,573	Via Filippo Maria Briganti	R	n.d	n.d
76	15/02/2014	4,519,547	432,352	Via Giulio Cesare, 119	R	5	2
77	16/02/2014	4,521,656	434,823	Via Mattia Preti	R	n.d	n.d

Table 1 (continued)

N	Date	WGS84—UTM-E	WGS84—UTM-N	Location	Factor	Diameter (m)	Depth (m)
78	19/02/2014	n.d	n.d	Via Marina	n.d	n.d	n.d
79	21/02/2014	4,521,113	435,713	Vai del Parco Margherita, 24 bis	R	n.d	n.d
80	01/04/2014	n.d	n.d	Fuorigrotta	n.d	n.d	n.d
81	04/04/2014	4,522,015	432,953	Via Paolo della Valle, 48	n.d	n.d	n.d
82	26/04/2014	n.d	n.d	Via Pigna	n.d	n.d	n.d
83	12/05/2014	4,518,809	430,485	Via Nuova Agnano, 2	R	n.d	n.d
84	12/05/2014	n.d	n.d	Via Marina	n.d	n.d	n.d
85	12/05/2014	n.d	n.d	Via San Giacomo	n.d	n.d	n.d
86	12/05/2014	n.d	n.d	Viale Traiano	n.d	n.d	n.d
87	12/05/2014	n.d	n.d	Via Epomeo	n.d	n.d	n.d
88	12/05/2014	4,523,372	435,844	Via Fontanelle	n.d	n.d	n.d
89	10/06/2014	4,523,289	436,216	Via Domenico di Gravina, 1–3	n.d	n.d	n.d
90	10/06/2014	n.d	n.d	Via Malaterra	n.d	n.d	n.d
91	12/06/2014	4,518,843	430,509	Via Nuova Agnano	n.d	< 1	n.d
92	12/06/2014	4,518,947	430,451	Via Nuova Agnano	n.d	n.d	n.d
93	15/09/2014	4,526,780	438,324	Viale delle Galassie, 23	n.d	< 2	n.d
94	18/11/2014	n.d	n.d	Via Casacelle, Giugliano	n.d	n.d	n.d
95	05/12/2014	n.d	n.d	Località Pantano	n.d	n.d	n.d
96	11/12/2014	4,526,214	435,733	Via Vincenzo Janfolla, 276	R	< 2	n.d
97	20/01/2015	4,523,064	435,980	Vico Delle Trone, 14	R	< 2	n.d
98	04/02/2015	4,523,661	436,258	Via Giuseppe Buonomo, 24	n.d	n.d	n.d
99	04/02/2015	4,524,679	435,840	Viale Colli Aminei, 30–50	A	3	1
100	16/02/2015	4,521,941	436,243	Vico Trinità delle Monache	n.d	n.d	n.d
101	21/02/2015	4,523,053	435,898	Vico delle Trone, 8	n.d	n.d	n.d
102	22/02/2015	4,522,542	430,650	Via Vicinale Campanile, 135	R	10	10

Table 1 (continued)

N	Date	WGS84—UTM-E	WGS84—UTM-N	Location	Factor	Diameter (m)	Depth (m)
103	24/02/2015	4,524,436	435,097	Viale Colli Aminei, 122	R	n.d	n.d
104	26/02/2015	4,523,415	436,739	Piazza Sanità	A	n.d	n.d
105	06/03/2015	4,520,851	434,834	Via Pontano, 41	n.d	n.d	n.d
106	06/03/2015	4,526,466	436,318	Via Janfolla, 476	n.d	n.d	n.d
107	12/03/2015	4,518,630	432,578	Via Manzoni	n.d	n.d	n.d
108	18/03/2015	4,522,435	436,103	C.so Vittorio Emanuele, 460—466	n.d	n.d	n.d
109	18/03/2015	4,523,492	429,714	Via Pallucci	n.d	0.5	0.5
110	25/03/2015	4,524,676	435,841	Viale Colli Aminei, 40/d	A	n.d	n.d
111	30/03/2015	4,521,401	436,649	Via Toledo/Vico Lungo Gelso	n.d	0.5	0.5
112	07/04/2015	4,525,220	434,851	Via Marco Rocco di Torrepadula	R	3	1.5
113	21/04/2015	4,524,675	435,844	Viale Colli Aminei, 40/d	n.d	n.d	n.d
114	04/05/2015	4,524,676	435,846	Viale Colli Aminei, 40/d	n.d	n.d	n.d
115	05/05/2015	4,525,208	434,816	Via Marco Rocco di Torrepadula	R	n.d	n.d
116	15/05/2015	4,519,272	433,661	Via Francesco Petrarca, 175	n.d	n.d	n.d
117	29/05/2015	4,524,846	438,075	Via Ponti Rossi, 250	R	n.d	n.d
118	03/07/2015	4,522,550	430,662	Via Vicinale Campanile, 131	R	n.d	n.d
119	03/07/2015	4,520,467	434,779	Riviera di Chiaia/Vico Antonio Serra	n.d	n.d	n.d
120	03/07/2015	n.d	n.d	Via Russolillo	R	n.d	n.d
121	20/07/2015	4,524,677	435,844	Viale Colli Aminei, 40/d	n.d	n.d	n.d
122	17/08/2015	4,525,208	434,822	Via Marco Rocco di Torrepadula	R	n.d	n.d
123	02/09/2015	n.d	n.d	Vico Soprammuro	n.d	n.d	n.d
124	24/09/2015	n.d	n.d	Via Russolillo	n.d	n.d	n.d
125	17/10/2015	4,518,551	429,718	Piazzetta Giusso	S	2	n.d
126	23/10/2015	4,519,644	431,944	Piazzale Tecchio	T	17	3
127	29/10/2015	n.d	n.d	Via Russolillo	A/S	n.d	n.d

Table 1 (continued)

N	Date	WGS84—UTM-E	WGS84—UTM-N	Location	Factor	Diameter (m)	Depth (m)
128	18/11/2015	4,527,026	436,187	Piscinola, direzione Capodichino	n.d	1	1
129	09/12/2015	4,523,593	437,604	Vico S. Maria Angeli alle Croci, 28	n.d	n.d	n.d
130	11/12/2015	4,524,160	427,833	Stazione Pisani della Circumflegrea	n.d	n.d	n.d
131	26/12/2015	4,524,460	435,540	Viale Colli Aminei, 68	A/S	n.d	n.d
132	26/12/2015	4,524,428	435,489	Via Nicolardi, 2	A/S	n.d	n.d
133	///2015	4,519,136	432,992	Via Manzoni, 157 a/b	n.d	1	n.d
134	26/01/2016	4,526,933	438,294	Parco San Gaetano Errico	A	< 2	n.d
135	13/02/2016	4,522,291	435,054	Via Tino di Camaino	n.d	n.d	n.d
136	20/02/2016	4,521,843	435,123	Via Enrico Alvino, 105–77	R	< 1	n.d
137	16/09/2016	4,523,962	434,175	Via Leonardo Bianchi, 3	R	n.d	n.d
138	17/09/2016	n.d	n.d	Via Concezione a Montecalvario	R	n.d	n.d
139	29/10/2016	4,523,594	436,638	Rampe San Gennaro dei Poveri	R	n.d	n.d
140	26/11/2016	4,523,219	438,790	Piazza Nazionale, 75	n.d	n.d	n.d
141	10/12/2016	4,521,581	435,296	Via Domenico Cimarosa, 56b	n.d	n.d	n.d
142	12/12/2016	4,523,931	434,802	Via Antonio Cardarelli, 16	R	n.d	n.d
143	12/12/2016	4,523,934	434,812	Cardarelli	R	n.d	n.d
144	12/12/2016	4,523,926	434,777	Via Cardarelli	n.d	n.d	n.d
145	04/05/2017	4,524,867	436,691	Via Gaetano Manfredi, 6	R	< 1	n.d
146	24/05/2017	4,523,895	434,353	Via Sergio Pansini, 511	S	n.d	n.d
147	18/06/2017	4,526,135	436,718	Via Miano	R	2	1
148	07/09/2017	4,521,641	432,005	Via Adriano, 10	R	3	n.d
149	08/09/2017	4,526,250	436,710	Via Miano	n.d	3	n.d
150	11/09/2017	4,522,890	438,886	Corso Meridionale, 47	R/T	n.d	n.d
151	11/09/2017	4,522,871	438,878	Corso Meridionale, 44/45	R	n.d	n.d
152	12/09/2017	4,523,224	434,468	Via San Giacomo dei Capri, 82	R	2	n.d

Table 1 (continued)

N	Date	WGS84—UTM-E	WGS84—UTM-N	Location	Factor	Diameter (m)	Depth (m)
153	12/09/2017	4,522,785	434,643	Via San Giacomo dei Capri, 43	R	1	n.d
154	14/09/2017	4,520,838	434,996	Via Francesco Crispi, 98	n.d	n.d	n.d
155	14/09/2017	4,520,819	435,010	Via Francesco Crispi, 81	n.d	n.d	n.d
156	22/09/2017	4,522,600	436,896	Via Broggia, 24	n.d	n.d	n.d
157	06/10/2017	4,523,465	430,186	Traversa II Provinciale di Napoli, 19	R	n.d	n.d
158	07/11/2017	4,520,822	435,000	Via Francesco Crispi, 98	R	< 1	n.d
159	02/12/2017	4,521,197	433,163	Via Po, 69	R	n.d	n.d
160	09/12/2017	4,517,091	433,062	Via Ferdinando Russo, 9	A	5	1
161	12/12/2017	4,523,040	437,095	Via Antonio Villari, 29	R	< 10	n.d
162	15/12/2017	4,519,979	432,613	Via Lepanto	A/S	n.d	n.d
163	30/12/2017	4,522,427	430,609	Via Montagna Spaccata, 234	n.d	n.d	n.d
164	23/01/2018	4,519,600	432,428	Via Giulio Cesare, 113	R	2	n.d
165	05/02/2018	4,523,247	430,165	Via Vicinale Trencia	R	n.d	n.d
166	20/02/2018	4,525,357	436,149	Via Nuova San Rocco	R	n.d	n.d
167	20/02/2018	n.d	n.d	Via Emilio Scaglione	n.d	n.d	n.d
168	23/02/2018	4,523,934	438,768	Via Generale Pianell	S	n.d	n.d
169	06/03/2018	4,522,321	434,192	Via Pigna, 130	R	2	n.d
170	18/03/2018	4,522,747	435,162	Via Pietro Platania, 6	R	n.d	n.d
171	20/03/2018	n.d	n.d	Via Giulio Palermo	n.d	n.d	n.d
172	21/03/2018	n.d	n.d	Via S. Biagio dei Librai	n.d	n.d	n.d
173	02/04/2018	4,519,270	433,207	Via Alessandro Manzoni, 141–145	n.d	n.d	n.d
174	10/04/2018	4,522,321	434,181	Via Pigna, 149	A/S	n.d	n.d
175	11/04/2018	n.d	n.d	Vico Politi	n.d	n.d	n.d
176	12/04/2018	n.d	n.d	Parco San Paolo	S	n.d	n.d
177	19/04/2018	4,523,225	434,469	Via San Giacomo dei Capri, 82	T	1	n.d

Table 1 (continued)

N	Date	WGS84—UTM-E	WGS84—UTM-N	Location	Factor	Diameter (m)	Depth (m)
178	24/04/2018	4,518,907	430,827	Via Diocleziano, 400	n.d	< 1	n.d
179	30/04/2018	4,518,911	430,832	Via Diocleziano, 249–251	S	n.d	n.d
180	27/07/2018	4,522,029	436,833	Via Domenico Capitelli, 30	R	< 1	n.d
181	22/08/2018	n.d	n.d	Via Marano Pianura	n.d	n.d	n.d
182	23/08/2018	4,526,239	433,635	Via del Cimitero, 572	R	n.d	n.d
183	12/10/2018	4,521,473	433,263	Via Piave. 232	n.d	n.d	n.d
184	30/10/2018	4,519,441	434,183	Largo Sermoneta	n.d	1	n.d
185	07/11/2018	4,524,618	436,556	Viale Colli Aminei, 21	n.d	n.d	n.d
186	18/11/2018	4,522,290	436,278	Via Ventaglieri, 28	n.d	n.d	n.d
187	06/01/2019	4,523,506	434,167	Via Onofrio Fragnito, 52	n.d	n.d	n.d
188	05/02/2019	4,519,915	432,533	Via Lepanto, 27	A/S	n.d	n.d
189	14/02/2019	4,518,577	433,087	Via Petrarca, 101	n.d	n.d	n.d
190	15/02/2019	4,522,313	435,651	P. Leonardo—Via Girolamo Santacr	n.d	1	n.d
191	18/02/2019	n.d	n.d	San Gregorio Armeno	n.d	n.d	n.d
192	20/03/2019	4,523,369	435,843	Via Fontanelle	n.d	n.d	n.d
193	24/03/2019	4,522,810	437,234	Ospedale S. Maria degli Incurabili	n.d	5	3
194	06/04/2019	4,522,813	437,232	Ospedale S. Maria degli Incurabili	n.d	n.d	n.d
195	13/04/2019	4,520,754	436,774	Galleria Vittoria—Via Acton	R	n.d	n.d
196	15/04/2019	n.d	n.d	Via Reggia di Portici	n.d	n.d	n.d
197	24/04/2019	4,520,267	432,636	Via Gabriele Rossetti, 15–46	T	n.d	n.d
198	17/05/2019	4,521,543	437,340	Via Alcide De Gasperi	n.d	n.d	n.d
199	25/05/2019	4,522,433	436,097	Corso Vittorio Emanuele, 486	R	n.d	n.d
200	29/05/2019	4,527,345	434,227	Via Cupa Spinelli	R	n.d	n.d
201	11/06/2019	n.d	n.d	Via Galeota	n.d	n.d	n.d
202	09/07/2019	4,517,386	432,689	Via Belsito	n.d	n.d	n.d

Table 1 (continued)

N	Date	WGS84—UTM-E	WGS84—UTM-N	Location	Factor	Diameter (m)	Depth (m)
203	11/07/2019	4,525,210	434,823	Via Marco Rocco di Torrepadula	R	n.d	n.d
204	17/07/2019	4,521,532	434,973	Via Luca Giordano, 30	A/S	n.d	n.d
205	20/07/2019	4,522,547	430,652	Via Campanile (traversa IV)	R	n.d	n.d
206	23/09/2019	4,527,636	434,330	Via Francesco Spinelli, 20	R	1	n.d
207	23/09/2019	4,522,777	436,710	Via Salvator Rosa, altezza Museo	R	n.d	n.d
208	28/09/2019	4,523,172	443,466	Via Immacolata Concezione	n.d	> 1	n.d
209	02/10/2019	4,521,895	436,242	Corso Vittorio Emanuele	n.d	n.d	0.3
210	07/10/2019	n.d	n.d	Corso Meridionale	R	n.d	n.d
211	15/10/2019	4,523,535	438,121	Via Michele Morelli	R	n.d	n.d
212	16/10/2019	4,524,979	433,590	Via Com. Santacroce ad Orsolone,	S	10	3
213	06/11/2019	4,524,948	433,591	Via Comunale Santacroce, 7ab	R	n.d	n.d
214	08/11/2019	4,520,621	436,272	Viale Calascione, 11/16	R	n.d	n.d
215	10/11/2019	4,526,805	436,612	Cupa Grande	A	n.d	n.d
216	12/11/2019	4,525,219	438,124	Via Udalrigo Masoni	R	4	n.d
217	13/11/2019	4,520,227	434,513	Piazza Gramsci	A/S	< 10	5
218	13/11/2019	4,525,410	438,149	Via Masoni	R	n.d	n.d
219	15/11/2019	4,520,724	442,385	Via delle Repubbliche Marinare	R	< 2	n.d
220	15/11/2019	4,522,448	435,103	Via Giotto	R	n.d	n.d
221	17/11/2019	n.d	n.d	Via Toscanini	R	n.d	n.d
222	17/11/2019	4,520,393	435,612	Via Caracciolo, 214	R	n.d	n.d
223	19/11/2019	4,519,316	431,759	Via Diocleziano	n.d	n.d	n.d
224	19/11/2019	4,523,256	435,256	Vico Molo alle due Porte	R	4	2
225	20/11/2019	4,521,947	432,517	Via dell'Epomeo, 244	R	3	0.5
226	21/11/2019	n.d	n.d	Via Camillo Guerra	R	n.d	n.d
227	21/11/2019	n.d	n.d	Via Leonardo Bianchi	R	n.d	n.d

Table 1 (continued)

N	Date	WGS84—UTM-E	WGS84—UTM-N	Location	Factor	Diameter (m)	Depth (m)
228	23/11/2019	4,526,600	436,624	Via Vincenzo Janfolla	R	3	n.d
229	24/11/2019	4,524,232	431,605	Via Mandracchio a Nazareth, 16	R	1	n.d
230	26/11/2019	4,518,587	432,558	Via Manzoni	R	n.d	n.d
231	29/11/2019	n.d	n.d	Via Com. Santacroce ad Orsolone	S	n.d	n.d
232	30/11/2019	n.d	n.d	Vico Banchi Nuovi	n.d	1	1
233	18/12/2019	4,520,063	432,240	Via Pietro Jacopo De Gennaro	n.d	> 2	2
234	21/12/2019	4,521,338	444,451	Via Bartolo Longo, 260	R	n.d	n.d
235	23/12/2019	4,525,208	434,795	Via Marco Rocco di Torrepadula	R	n.d	n.d
236	13/01/2020	4,524,233	431,608	Via Mandracchio a Nazareth, 16	n.d	n.d	n.d
237	12/03/2020	4,522,278	436,298	Via Ventaglieri, 24	A	n.d	n.d
238	09/05/2020	4,523,067	444,623	Viale Carlo Miranda	n.d	n.d	n.d
239	10/06/2020	4,522,107	437,946	Vico Campane a S. Eligio	n.d	n.d	n.d
240	15/07/2020	4,526,647	436,569	Via vecchia comunale Piscinola	R	< 1	n.d
241	27/07/2020	4,527,026	433,545	Via Cupa Fragolara	A	15	6
242	04/08/2020	4,527,025	433,537	Via Cupa Fragolara	A	n.d	n.d
243	29/09/2020	4,526,647	436,569	Via vecchia comunale Piscinola	R	< 1	n.d
244	??/10/2020	4,522,127	432,804	Via Quattro Novembre 56	R	1	n.d
245	05/10/2020	4,522,005	432,259	Via dell'Epomeo, 348	R	n.d	n.d
246	12/10/2020	4,516,996	431,464	Via Tito Lucrezio Caro, 6	R	n.d	n.d
247	27/10/2020	4,519,955	432,800	Via Giacomo Leopardi, 32	R/S	n.d	n.d
248	17/11/2020	4,522,473	434,433	Via Pigna, 228	R	n.d	n.d
249	17/11/2020	4,522,810	435,576	Piazza Canneto, 2	R	2	n.d
250	02/12/2020	n.d	n.d	Scampia-Mugnano	R	n.d	n.d
251	07/12/2020	4,524,812	433,638	Monaldi	R	n.d	n.d
252	02/01/2021	4,527,597	435,548	Via Tancredi Galimberti	n.d	< 1	n.d

Table 1 (continued)

N	Date	WGS84—UTM-E	WGS84—UTM-N	Location	Factor	Diameter (m)	Depth (m)
253	02/01/2021	4,527,603	435,539	Via Tancredi Galimberti	n.d	< 1	n.d
254	08/01/2021	n.d	n.d	Via Coroglio	R	n.d	n.d
255	08/01/2021	4,522,618	444,900	Ospedale del Mare—Parcheggio	R	50	20
256	08/01/2021	4,522,590	444,984	Str. Vic.le Cupa Pironti	S	1	1
257	08/01/2021	4,521,831	434,276	Via Pietro Mascagni, 53	R	< 1	n.d
258	10/01/2021	4,524,483	431,881	Via Com. Guantai ad Orsolone, 184	R	n.d	4
259	12/01/2021	4,522,597	444,057	Via Angelo Camillo de Meis, 175	n.d	n.d	n.d
260	20/01/2021	4,526,126	438,638	Strada Comunale del Cassano, 47	R	n.d	n.d
261	03/02/2021	4,524,264	437,871	Via Martin Luther King, 12—Napoli	n.d	0.4	0.5
262	11/02/2021	4,526,226	433,608	Via Comunale Margherita	A	n.d	n.d
263	22/02/2021	4,526,642	436,399	Via Teano, 40/46	A	4	1
264	08/03/2021	4,521,399	434,838	Via Aniello Falcone, 88	T	1.5	n.d
265	16/03/2021	4,518,388	432,455	Via Alessandro Manzoni, 209	A	n.d	n.d
266	13/04/2021	4,521,982	435,298	Via Michele Kerbaker, 146	R	1	n.d
267	14/05/2021	4,523,571	437,162	vico San Marco a Miradois	R	20	10
268	15/06/2021	4,520,890	434,692	Corso Vittorio Emanuele	n.d	n.d	n.d
269	17/06/2021	n.d	n.d	Via Roma, 65	nd	2	3
270	///01/2021	4,523,259	438,550	Via Arenaccia, 45	n.d	0.8	1

For each event are indicated (in known): identification number, date (dd/mm/yyyy) of sinkhole occurrence; coordinates (WGS84); triggering factors recognised; diameter (in m); depth (in m)

A Aqueduct leak, *R* rainfall, *S* sewer leak, *W* water infiltration, *T* vehicular traffic, *n.d.* not defined

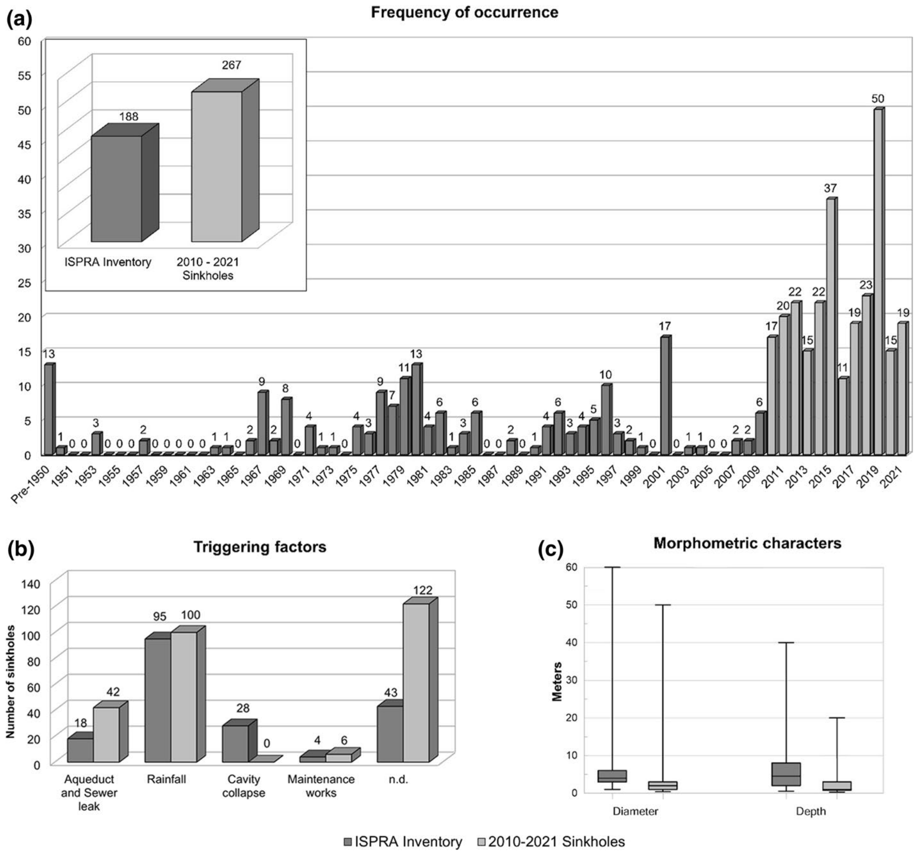

Fig. 4 **a** Annual sinkhole frequency (number of events per year) from the middle of the last century (data prior than 1950 have been represented as a single data value) to June 2021; **b** Triggering factors; **c** Statistical representation of known diameters and depths for 2010–2021 and ISPRA inventories

ISPRA inventory classified 28 events as triggered by cavity-roof collapse. In our case we consider the cavity-roof collapse as a genetic process and not as a triggering factor: therefore, no updated sinkhole falls in this class. Finally, morphometric characters show differences in the median value as well as in the general distribution (Fig. 4c). In particular, with respect to ISPRA inventory, diameter and depth of the new data are smaller and included in a narrower range.

4.2 Characteristics of newly inventoried sinkholes

The yearly frequency (number of events per year) of the new 267 inventoried events of known timing of occurrence (Fig. 4a) indicates a rate between 11 and 23 events per year over the period of inventory updating. Exceptions are the 37 events recorded in 2015 and the 50 events recorded in 2019, so that about 32% of the 267 new events with known timing of occurrence (this datum is not available for 3 events) were triggered in these two years only. It is worth to point out that events referred to 2010 are only a part of the total, since they represent the events not already included in the ISPRA database. Similarly, for 2021 the data are incomplete, since they refer only to the first six months of the year.

As far as the triggering factors are concerned (Fig. 4b), for about 45% of the events the triggering factor is unknown. The remaining 55% can be associated to rainfall events (37% of the new addition), 15.6% occur due to leakage from underground aqueduct and sewer system, also connected to heavy rainstorms, while no direct correlation with seismic events is recorded, although some seismic events characterized by a medium to low intensity (earthquake duration magnitude M_d between 3.0 and 1.9—from National Institute of Geophysics and Volcanology, INGV) occurred in the time frame. A very small percentage of the cases (2.2%) are related to the action or weight of vehicles and materials used for road and maintenance works.

Morphometric data of sinkholes occurred between 2010 and 2021 are available for 80 events only (about 28.5%) as regards diameter and for 42 events (15%) for depth (Fig. 4c). Statistical analysis shows that diameter ranges between 0.4 and 50 m, but only 9 sinkholes have diameters greater than 5 m, while median value is 2 m. Depth ranges between few centimeters to 20 m, even if only 5 events have a depth greater than 5 m: in this case, the median value is 1 m. This consistency is in agreement with the types of sinkholes recognized: collapse sinkholes are commonly of metric size (e.g. Parise 2012, Gutièrrez et al. 2014), while sinkholes linked to the leak of aqueduct or sewer system are characterized by depths lower than one meter (e.g. Kim et al. 2018).

About data sources, 241 of the new sinkholes were derived by newspaper sources. Data on 78 events were collected through national newspapers, 163 events were collected through local newspapers and 15 through local council reports (e.g. Naples council) (Fig. 5), 14 additional events were collected by field survey, for a total of 270 new events.

The dataset of events for which coordinates of occurrence are known, consists of 380 sinkholes distributed over the study area (Table 1; Fig. 6a). Distribution of sinkholes is mainly concentrated in the central area that encompasses the ancient center of the city. The heat map indicating the number of sinkholes per km^2 (Fig. 6b) shows a concentration higher than 12 units per km^2 in this area of the city, which corresponds to the most important one in terms of cultural asset and vulnerability to sinkholes. In fact, here, a rich architectural heritage made up of castles, royal palaces, noble residences, cathedrals, churches, chapels and convents which, forming the cultural asset of the city, have contributed to the inclusion of the center of Naples in the list of UNESCO World Heritage sites in December 1995 (Clemente et al. 2015), are located. In the same area the most complex part of the system of underground cavities and tunnels is present. The higher concentration of sinkholes in the central sector of the city is also confirmed by analyzing the distribution of new inventoried sinkholes referred to the period February 2010–June 2021, and the related heat maps (Fig. 6c–f).

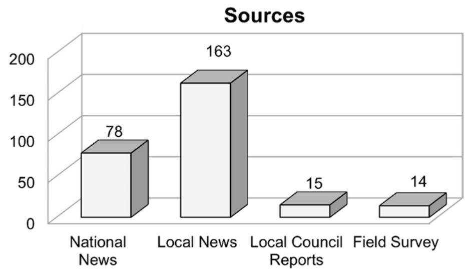

Fig. 5 Source of new 2010–June 2021 sinkhole data

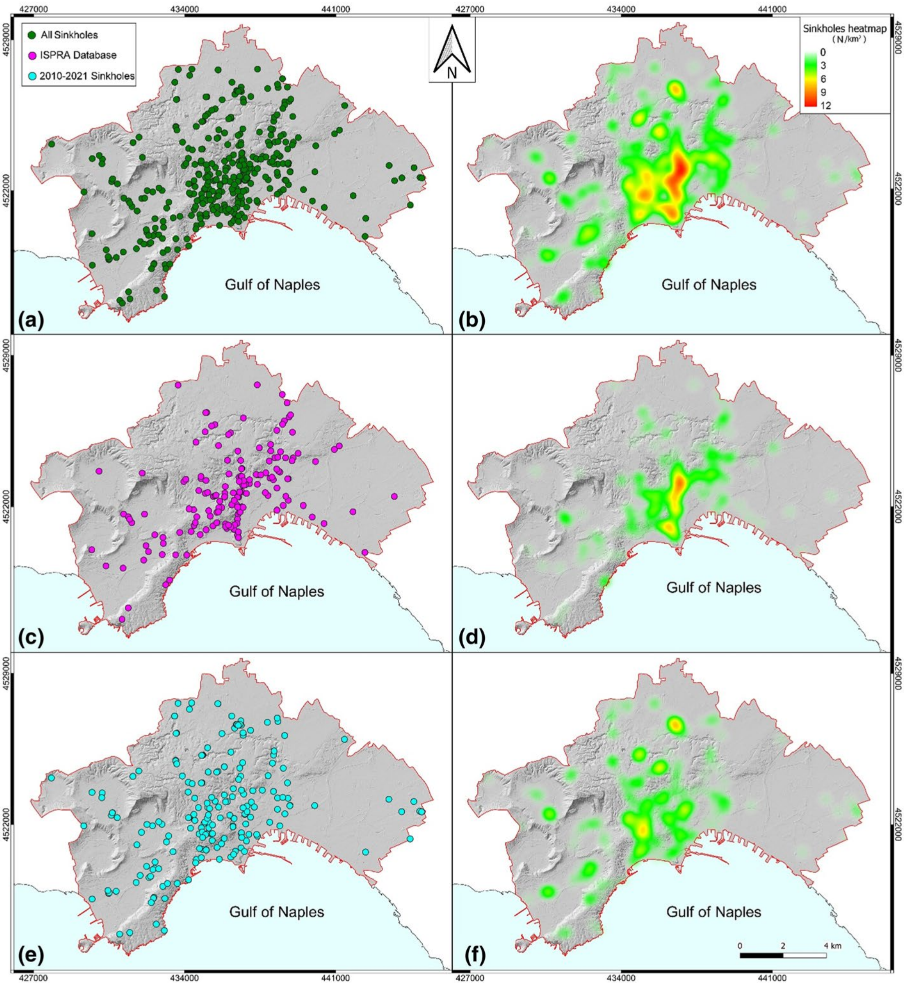

Fig. 6 **a** Updated sinkhole inventory map; **b** Heat map of the updated sinkhole inventory (n/km^2); **c** Sinkholes occurred from 1880 to 2010 as derived from ISPRA database (Guarino and Nisio, 2012); **d** Heat map of sinkholes (n/km^2) for the 1880–2021 time span; **e** Newly inventoried sinkholes occurred from 2010 to 2021; **f** Heat map of sinkholes occurred from 2010 to June 2021 (n/km^2)

Distribution analysis of sinkholes within the municipalities of the city of Naples was conducted considering both the events with known coordinates and streets of occurrence (Fig. 7). In this last case, in absence of house number, the event was considered only if the street fell entirely within a single municipality. In particular, the events inventoried by ISPRA with known coordinates were 167, while 11 sinkholes positions were derived from the information of the street of occurrence, for a total of 178 events with known position.

The new inventoried sinkholes referred to the period February 2010–June 2021 consists of 213 events with known coordinates and 42 events with position in the municipality derived from address information, for a total of 255 sinkholes.

In detail, between 1880 and 2010 most of the events (78%) occurred within the (1) municipality 1—Chiaia, Posillipo, S. Ferdinando, (2) municipality 2—Avvocata,

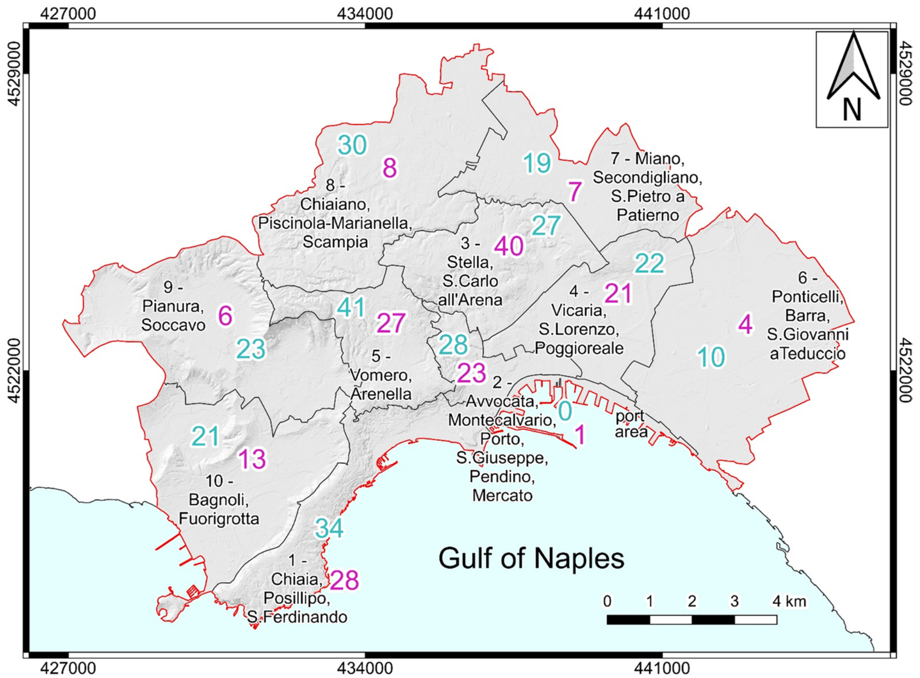

Fig. 7 Distribution of sinkholes for each municipality of Naples occurred between 1880 and 2010 (ISPRA database) in purple, and between 2010 and June 2021 in cyan

Montecalvario, Porto, S. Giuseppe, Pendino, Mercato, (3) municipality 3—Stella, S. Carlo all'Arena, (4) municipality 4—Vicaria, S. Lorenzo, Poggioreale and (5) municipality 5—Vomero, Arenella. Instead, between 2010 and 2021 almost 80% of the events occurred within the (1) municipality 1—Chiaia, Posillipo, S. Ferdinando, (2) municipality 2—Avvocata, Montecalvario, Porto, S. Giuseppe, Pendino, Mercato, (3) municipality 3—Stella, S. Carlo all'Arena, (4) municipality 4—Vicaria, S. Lorenzo, Poggioreale, (5) municipality 5—Vomero, Arenella, (6) municipality 8—Chiaiano, Piscinola-Marianella, Scampia, (7) municipality 10—Bagnoli, Fuorigrotta. Such distribution confirms the trend of sinkholes trigger in the central sector of the city, but highlights an enlargement of the involved area in the most recent years.

4.3 Sinkhole susceptibility analysis

The fraction of the inventory for which coordinates of occurrence are known was used to produce a preliminary sinkhole susceptibility map for the city of Naples using the Frequency Ratio approach. Frequency Ratio scores indicate a heavy influence of Underground Cavities Density and, subordinately, of Distance. Underground Railroad Density appears as the most important predisposing factor; conversely, Groundwater Depth, Cover Thickness and Road Network Density are the least important ones. Sinkhole susceptibility map shows the spatial distribution of very high susceptibility class mostly in the central area of the city of Naples: municipality 2 is almost entirely characterized by this susceptibility class, while municipalities 1, 3, 4, 5 and 10 only partially. Generally, susceptibility classes show a decreasing trend from the ancient centre of the city to the bordering areas (here from medium to very low) and reflect the pattern of the most important roads. The sinkhole susceptibility map (Fig. 8) was categorized into five classes: (1) very low, (2) low, (3) medium, (4) high, (5) very high, which correspond to 30%, 35%, 18%, 11% and 6% of the total area, respectively. The predictive performance analysis returns a ROC/AUC score equal to 0.81 (1.00 represents the maxima predictive performance).

5 Discussion

The updated inventory of the anthropogenic sinkholes of the city of Naples consists of 458 entries, 270 of which are newly identified sinkholes occurred in the period February 2010–June 2021. It represents an update of the previous available inventory (ISPRA, Guarino and Nisio 2012), that consisted of 188 sinkholes collected in the time interval from 1880 until 2010. Overall, new sinkholes are present in all of the municipalities of the city with a time-growing trend compared to ISPRA database in the bordering municipalities. The highest concentration is located in the municipalities 2 and 5 and significant concentrations are present in municipalities 1 and 3 (Fig. 9). The analysis of sinkhole inventory highlights an increasing trend in the annual frequency of sinkholes (Fig. 10).

From the analysis of number of sinkholes cumulated over the time it is possible to notice a regular growth of the events until 2011 and a subsequent abrupt increase in the last decade, coinciding with the inventory update. Although this might be related to the higher availability of data source, a relation with the rapid settlement development occurred in the

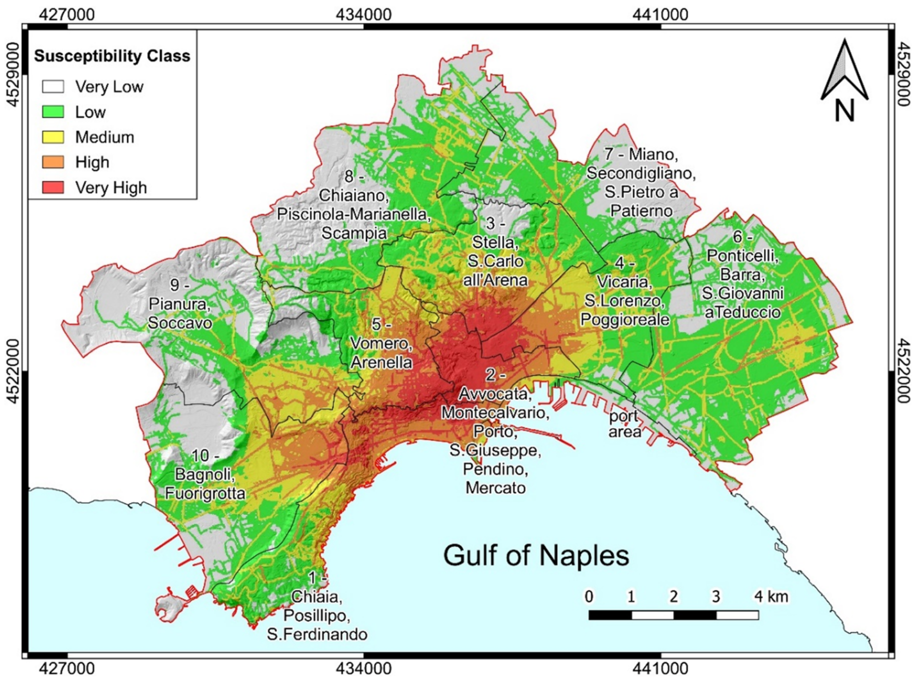

Fig. 8 Sinkhole susceptibility map

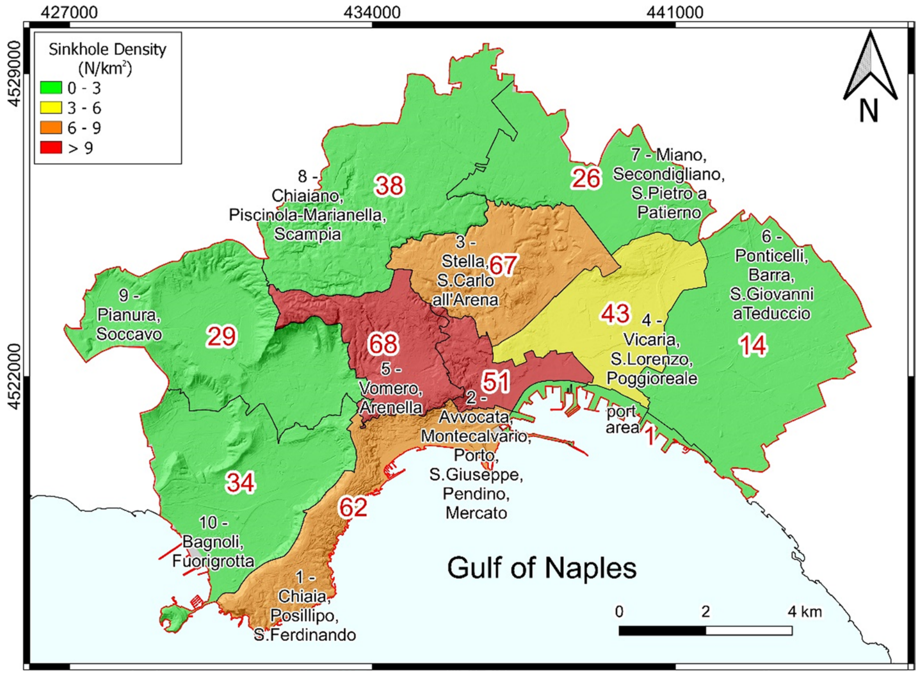

Fig. 9 Average density of sinkholes for each municipality of Naples

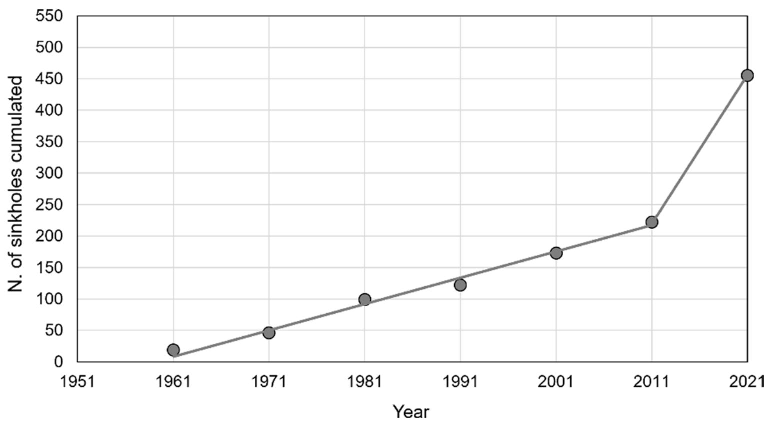

Fig. 10 Cumulative distribution of sinkholes from 1961 to 2021

past decades that led to an increase of aqueduct demand and sewer systems use (frequently inadequate with damage and/or leakage), cannot be excluded.

Geological setting of the study area has also an influence on sinkholes development. In fact, sinkholes are concentrated in the central area of the city coinciding with its ancient centre, where NYT formation is present in the subsoil and is characterized by diffuse underground cavities that sometimes undergo roof collapses (Nicotera and Lucini 1967; Albertini et al. 1988; Evangelista et al. 2002; Lombardi et al. 2010; Basso et al. 2013).

Even if the Frequency Ratio analysis for sinkholes susceptibility assessment highlights that the cover thickness and consequently the depth of NYT does not represent one of the most important predisposing factor, water losses from aqueduct and sewer systems coupled with the water infiltration action and the weathering processes can be associated to the progressive degradation of mechanical properties of NYT. In the opposite, sinkholes are less frequent in the other sectors of the city, where the network of cavities is much more sporadic: this occurs in the eastern sector, where prevailingly loose, non-volcanic materials are present (hence, not suitable as building materials) and western one, strongly affected by tectonic-volcanic collapse event in the past that makes hard the excavation of the material. Sinkholes susceptibility map confirms the medium-very low susceptibility degrees of these sector of the city, in agreement with previous studies (e.g. Guarino and Nisio 2012; Basso et al. 2013). Differently, susceptibility presents significant difference in the northern and south-east sectors of the city, in past classified as very high-medium susceptibility. Such differences, confirming the importance of an updated sinkhole inventory for supporting susceptibility analysis.

Anthropogenic sinkholes which affect Naples are also present in the hinterland of the city (Guarino et al. 2018; Scotto di Santolo et al. 2018) where preexisting network of caves within the Campanian Ignimbrite tuff at shallow depths is historically subject to sinkhole formation. Similarly, in the urban area of Rome (Italy), tunnels produced by historical mining activities of tuffs and pyroclastic rocks, drainage tunnels and catacombs, can easily predispose the collapse of the deeper layers. Furthermore, runoff activity concurrently with intense rainfall can lead to the loose of soil below the road surface, causing the collapse of the shallow layers (Ciotoli et al. 2013). Naples' sinkholes present similarities with those occurring over the world, both in areas characterized by past quarrying of soluble or soft rocks, such as in Netherlands, USA and Korea (Bekendam 1998; Galloway et al. 1999; Sunwoo et al. 2010) and in areas characterized by obsolete or defective sewer pipes, as in Guatemala, Japan and South Korea (Hermosilla 2012; Yokota et al. 2012; Kim et al. 2018).

The genetic mechanism of sinkholes was analyzed comparing sinkholes' distribution with those of cavities, in the form of 30 m-buffered polygons to minimize the effects of the lack of knowledge for some cavities in size and extension and according to the Frequency Ratio scores which indicate the heavy predisposing influence of Underground Cavities Density. The results show 41 events that fall inside the buffered area (Fig. 11a). Such events, representing almost 20% of the 213 new sinkholes with known coordinates,

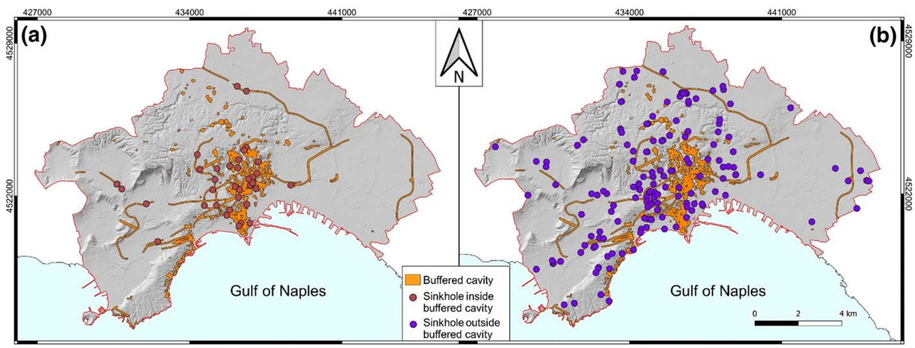

Fig. 11 **a** Distribution of sinkholes falling inside the 30 m-buffered cavity; **b** Distribution of sinkholes falling outside the 30 m-buffered cavity

can be classified as collapse. Such fraction is close to that estimated by Guarino and Nisio (2012) for the old inventory, for which the collapse was identified as triggering mechanism in around 25% of the total cases. The remaining 80% of the new sinkholes are distributed over a larger area and do not fall within buffered cavities (Fig. 11b). These sinkholes (or part of them) could be associated to sewerage system-induced sinkholes (Rogers 1986), linked to groundwater or sewer infiltration through a damaged sewer pipe, especially during and after a heavy rainfall (Kim et al. 2018). The discharge of soil particles related to the action of water infiltration leads to loosening of the soil with formation of underground cavities, and ground collapse. However, it is important to remember that data on dimension and distribution of cavities in the subsoil of Naples could be unprecise and that the number of sinkholes originated by collapse mechanism could be underestimated.

Relations between sinkholes and presumable triggering factors have been deeply investigated (Fig. 12). Distribution of monthly aggregated rainfall data from January 2010 to June 2021 seems to be in good agreement with rainfall-induced sinkholes frequency. As highlighted in Sect. 4, years 2015 and 2019 were characterized by a higher number of sinkhole events. In particular, sinkholes occurred in 2015 are distributed during the entire year, with concentrations in correspondence of particularly rainy months (e.g. February and June). In the opposite, sinkholes occurred in 2019 are concentrated in November (almost half of all sinkholes occurred in the year), when the amount of rainfall is higher than the average for the period. In this specific month, 15 sinkholes are classified as triggered by rainfall, 3 as derived by aqueduct and sewer leaks and 2 by not defined factor (n.d.). It is important to underline that the sewer system considered is also responsible for disposal of water from road pavements and delivering it to the sea, whereby in cases of intense rainfall, leaks from sewer system make difficult to associate sinkhole formation to a specific triggering factor. A significant correlation between collapse mechanism and rainfall seems to exist. Indeed, a sort of clustering of collapse sinkholes in correspondence of wettest months was identified

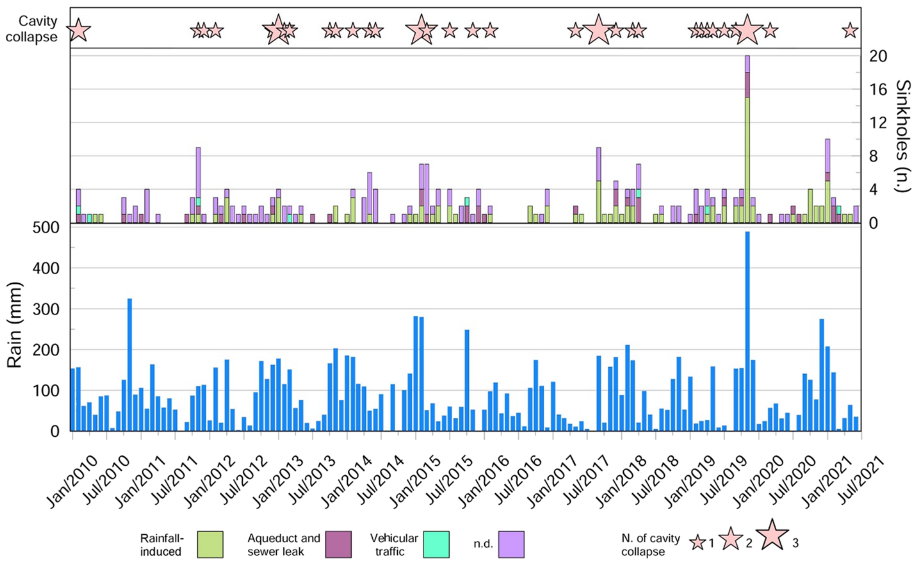

Fig. 12 Distribution of monthly cumulative rainfall, sinkholes divided for triggering factor; stars refer to number of sinkholes originated by cavity-collapse mechanism

(Fig. 12). This evidence might be explained considering that continuous and prolonged soaking, saturating the ground, represents a relevant factor promoting instability of cavity roof (e.g. Scotto di Santolo et al. 2018).

The knowledge of predisposing factors, such as the presence of underground network of cavities and distribution of sewer system, could represent an important basis in the development of a reliable sinkhole susceptibility analysis. In this perspective, because the location of cavities is partially unknown, a specific survey oriented to the identification and characterization (i.e. cavity's dimension, depth, filling etc.…) of such elements would be significant. Moreover, the identification of the most susceptible areas can be used in planning the inspection strategies. On these bases, monitoring systems for pore-pressure and/or deformation of cavity's roof as well as cavity stability analysis could be envisaged.

6 Conclusions

To improve the knowledge of anthropogenic sinkholes in the city of Naples in view of a prospective evaluation of hazard and risk, a new and updated inventory of sinkhole has been created and here presented. In particular, moving from an available inventory consisting of 188 sinkholes, events occurred between February 2010 and June 2021 were collected and characterized through newspaper analysis and field surveys. The new updated inventory now consists of 458 entries, 270 of which occurred after 2010. Information about date, location, triggering factor and morphometry have been derived from available sources and associated to the inventoried event. For its quantity of data, the inventory constructed in this study constitutes an exceptional volume of information and offers an excellent opportunity to develop significant prediction models in near future, considering not only the probability of occurrence of new sinkholes, but also magnitude and frequency relationships of the collapse events. However, an attempt to develop a preliminary sinkhole susceptibility assessment was done through the application of Frequency Ratio approach and considering twelve factors as predisposing to the sinkhole occurrence.

Database analysis reveals some important aspects: (1) annual frequency of the events has a sustained increasing trend; (2) statistical distribution of triggering factors and morphometric characters are consistent with previous studies; (3) spatial distribution of the new inventoried sinkholes coincides with the area of the city already affected by sinkholes in the past, even if a growing trend in the neighbouring areas of the city has been observed; (4) higher concentration of events is recognized in the ancient centre of the city where a diffuse network of cavities is present. This is also confirmed by sinkhole susceptibility map which identifies the most susceptible area coincident with the ancient centre of the city, while a medium–low susceptibility characterizes the outermost areas.

A matching analysis between sinkhole position and buffered cavities indicates that a fraction of the new inventoried sinkholes can be associated to a cavity-collapse mechanism, highlighting the role of such underground elements in promoting surface instabilities. As expected, and consistently with the existing inventory, a large fraction of sinkholes was triggered by rainfall events and aqueduct and sewer damage. However, the definition of the triggering mechanisms is very difficult or sometimes impossible (especially for old events). In this perspective, analysis of correlation between rainfall and sinkholes events deserves to be further investigated in the context of an evaluation of sinkholes risk, also posing particular attention to the distribution of aqueduct and sewer network that cross the city.

Acknowledgements The authors thank "Consorzio interUniversitario per la prevenzione dei Grandi Rischi (CUGRI)" for providing technological support, "Sintema Engineering srl" for *Cimitero delle Fontanelle* photo, the two anonymous reviewers for providing constructive reviews of the manuscript and the Editor for its editorial suggestions.

Funding Funding was provided by the Italian Ministry for Education, University and Research (MIUR-Italy), through 2017 PRIN Project "URGENT—Urban Geology and Geohazards: Engineering geology for safer, resilieNt and smart ciTies" (Project code 2017HPJLPW_005; CUP E68D17000200001; Principal Investigator: Domenico Calcaterra).

Data availability Data and materials are available under motivated request.

Declarations

Conflict of interest The authors have no conflicts of interest to declare that are relevant to the content of this paper.

References

Albertini V, Baldi A, Bartoli L, Collini F, Esposito C, Guerra V, Miraglino P, Schiattarella F, Vallario A (1988) Le cavità sotterranee del napoletano: pericolosità e possibili utilizzazioni. Geol Tec 3:54–63 (**in Italian**)

Allocca V, Angrisani AC, Coda S, Danzi M, De Vita P, Del Vecchio U, Di Martire D, Massa D, Minin G, Nocerino G, Calcaterra D (2018) 3D reconstruction through a lightweight hand-held laser scanner of an underground cavity located in the SS. Marcellino and Festo Monumental Complex (Napoli, Italy). In: Proceedings of the Cavità di origine antropica, modalità d'indagine, aspetti di catalogazione, analisi della pericolosità, monitoraggio e valorizzazione. Geologia dell'Ambiente, Periodico trimestrale della SIGEA. Supplemento al n 4/2018 (in Italian)

Amato L, Carsana V, Cinque A, Di Donato V, Giampaola D, Guastaferro C, Irollo G, Morhange C, Romano P, Ruello MR, Russo Ermolli E (2009) Ricostruzioni morfoevolutive nel territorio di Napoli: l'evoluzione tardo pleistocenica-olocenica e le linee di riva di epoca storica. Méditerranée 112:23–31 (**In Italian**)

Ammirati L, Mondillo N, Rodas RA, Sellers C, Di Martire D (2020) Monitoring land surface deformation associated with gold artisanal mining in the Zaruma City (Ecuador). Remote Sensing 12(13):2135. https://doi.org/10.3390/rs12132135

Basso N, Ciotoli G, Finoia MG, Guarino PM, Miraglino P, Nisio S (2013) Suscettibilità a fenomeni di sinkholes antropogenici nel territorio di Napoli. Mem Descr Carta Geol D'it 93:73–104 (**In Italian**)

Beck BF, Jenkins DT (1986) Geotechnical considerations of sinkhole development in Florida. In: International symposium of environmental geotechnology, p 8

Bekendam RF (1998) Pillar stability and large-scale collapse of abandoned room and pillar limestone mines in South-Limburg, the Netherlands. University of Utrecht (PhD thesis)

Bellucci F, Corniello A, De Riso R (1993) Geology and hydrogeology of the Somma-Vesuvio volcano (Southern Italy). IAH Memoires 24(1):137–149

Bétournay MC (2009) Abandoned metal mine stability risk evaluation. Risk Anal 29(10):1355–1370

Bonham-Carter GF (1994) Geographic information systems for geoscientists: modeling with GIS. Pergamon Press, Oxford, pp 398–403

Brancaccio L, Cinque A, Romano P, Rosskopf C, Russo F, Santangelo N, Santo A (1991) Geomorphology and neotectonic evolution of a sector of the Tyrrhenian flank of the Southern Apennines (Region of Naples, Italy). Zeitschrift Für Geomorphologie, Neue Folge 82:47–58

Brinkmann R, Parise M, Dye D (2008) Sinkhole distribution in a rapidly developing urban environment: Hillsborough County, Tampa Bay area. Florida Eng Geol 99(3–4):169–184

Cando Jácome M, Martinez-Graña AM, Valdés V (2020) Detection of Terrain deformations using InSAR techniques in relation to results on Terrain subsidence (Ciudad de Zaruma, Ecuador). Remote Sens 12(10):1598

Cennamo C, Angelillo M, Cusano C (2017) Structural failures due to anthropogenic sinkholes in the urban area of Naples and the effect of a FRP retrofitting. Compos B Eng 108:190–199. https://doi.org/10.1016/j.compositesb.2016.09.043
Choi JK, Kim KD, Lee S, Won JS (2010) Application of a fuzzy operator to susceptibility estimations of coal mine subsidence in Taebaek City, Korea. Environ Earth Sci 59:1009–1022
Cinque A, Irollo G, Romano P, Ruello MR, Amato L, Giampaola D (2011) Ground movements and sea level changes in urban areas: 5000 years of geological and archaeological record from Naples (Southern Italy). Quatern Int 232(1–2):45–55. https://doi.org/10.1016/j.quaint.2010.06.027
Ciotoli G, Corazza A, Finoia MG, Nisio S, Serafini R, Succhiarelli C (2013) Sinkholes antropogenici nel territorio di Roma Capitale. I Sinkholes: metodologie di indagine, ricerca storica, sistemi di monitoraggio e tecniche di intervento. Centri abitati e processi di instabilità naturale: valutazione, controllo e mitigazione. Mem Descr Carta Geol D'it 93:143–181 (**in Italian**)
Clemente M, Castagnaro A, Oppido S, Daldanise G (2015) Cultural heritage and collaborative urban regeneration: the Sansevero chapel museum for the historic centre of Naples. BDC Bollettino Del Centro Calza Bini 15(1):93–112
D'Argenio B, Pescatore T, Scandone P (1973) Schema geologico dell'Appennino meridionale (Campania e Lucania). Atti del Conv. Moderne vedute sulla geologia dell'Appennino. Acc Nazion Lincei 182:49–72 (**In Italian**)
Del Prete S, Iovine G, Parise M, Santo A (2010) Origin and distribution of different types of sinkholes in the plain areas of Southern Italy. Geodin Acta 23(1–3):113–127. https://doi.org/10.3166/ga.23.113-127
Dixon SJ, Viles H, Garrett B (2018) Ozymandias in the anthropocene: the city as an emerging landform. Area 50:117–125. https://doi.org/10.1111/area.12358
Evangelista A, Aversa S, Pescatore TS, Pinto F (2000) Soft rocks in southern Italy and role of volcanic tuffs in the urbanization of Naples. In: Proceedings of the II international symposium on 'The Geotechnics of Hard Soils and Soft Rocks', Napoli, vol 3, pp 1243–1267
Evangelista A, Flora A, Lirer S, De Sanctis F, Lombardi G (2002) Studi ed interventi per la tutela di un patrimonio sotterraneo: l'esempio delle cavità di Napoli. L'Aquila, XXI Convegno Nazionale di Geotecnica, Patron Ed., Bologna, pp 579–588 (in Italian)
Fazio NL, Perrotti M, Lollino P, Parise M, Vattano M, Madonia G, Di Maggio C (2017) A three-dimensional back-analysis of the collapse of an underground cavity in soft rocks. Eng Geol 228:301–311. https://doi.org/10.1016/j.enggeo.2017.08.014
Galeazzi C (2013) The typological tree of artificial cavities: a contribution by the Commission of the Italian Speleological Society. Opera Ipogea 1:9–18
Galloway D, Jones DR, Ingebritsen SE (1999) Land sunbsidence in the United States, vol 1182. U.S. Geological Survey. Circular, Reston.
Galve J, Gutiérrez F, Lucha P, Guerrero J, Bonachea J, Remondo J, Cendrero A (2009) Probabilistic sinkhole modelling for hazard assessment. Earth Surf Proc Land 34:437–452
Gao Y, Luo W, Jiang X, Lei M, Dai J (2013) Investigations of large scale sinkhole collapses, Laibin, Guangxi, China. In: Proceedings of the 13th multidisciplinary conference on sinkholes and the engineering and environmental impacts of karst: NCKRI symposium 2, pp 327–331
Guarino PM, Nisio S (2012) Anthropogenic sinkholes in the territory of the city of Naples (Southern Italy). Phys Chem Earth Parts a/b/c 49:92–102. https://doi.org/10.1016/j.pce.2011.10.023
Guarino PM, Santo A, Forte G, De Falco M, Niceforo DMA (2018) Analysis of a database for anthropogenic sinkhole triggering and zonation in the Naples hinterland (Southern Italy). Nat Hazards 91(1):173–192. https://doi.org/10.1007/s11069-017-3054-5
Gutiérrez F, Cooper AH, Johnson KS (2008) Identification, prediction and mitigation of sinkhole hazards in evaporite karst areas. Environ Geol 53:1007–1022. https://doi.org/10.1007/s00254-007-0728-4
Gutiérrez F, Parise M, De Waele J, Jourde H (2014) A review on natural and human-induced geohazards and impacts in karst. Earth Sci Rev 138:61–88. https://doi.org/10.1016/j.earscirev.2014.08.002
Hatzor YH, Talesncik M, Tsesarsky M (2002) Continuous and discontinuous stability analysis of the bell-shaped caverns at Bet Guvrin, Israel. Int J Rock Mech Min Sci 39:867–886
Heidari M, Khanlari GR, Beydokhti AT, Momeni AA (2011) The formation of cover collapse sinkholes in North of Hamedan. Iran Geomorphol 132(3–4):76–86. https://doi.org/10.1093/acrefore/9780199389407.013.40
Hermosilla RG (2012) The Guatemala City sinkhole collapses. Carbonates Evaporites 27(2):103–107
Iovine G, Vennari C, Gariano SL, Caloiero T, Lanza G, Nicolino N et al (2016) The "Piano dell'Acqua" sinkholes (San Basile, Northern Calabria, Italy). Bull Eng Geol Env 75(1):37–52
ISTAT (2019) Censimento della popolazione del 2011. http://censimentopopolazione.istat.it/. (in Italin)
Jenks GF (1967) The data model concept in statistical mapping. Int Yearbook Cartogr 7:186–190

Jiang X, Lei M, Li Y, Dai J (2005) National-scale risk assessment of sinkhole hazard in China. In: Sinkholes and the engineering and environmental impacts of Karst, pp 649–658
Karimi H, Taheri K (2010) Hazards and mechanism of sinkholes on Kabudar Ahang and Famenin plains of Hamadan. Iran Nat Hazards 55(2):481–499. https://doi.org/10.1007/s11069-010-9541-6
Kim KD, Lee S, Oh HJ, Choi JK, Won JS (2006) Assessment of ground subsidence hazard near an abandoned underground coal mine using GIS. Environ Geol 50:1183–1191
Kim KD, Lee S, Oh HJ (2009) Prediction of ground subsidence in Samcheok City, Korea using artificial neural networks and GIS. Environ Geol 58:61–70
Kim YJ, Xiao H, Wang D, Choi YW, Nam BH (2017) Development of sinkhole hazard mapping for Central Florida. Geotech Front 2017:459–468
Kim K, Kim J, Kwak TY, Chung CK (2018) Logistic regression model for sinkhole susceptibility due to damaged sewer pipes. Nat Hazards 93(2):765–785
Lei M, Gao Y, Jiang X, Hu Y (2005) Experimental study of physical models for sinkhole collapses in Wuhan, China. In: Sinkholes and the engineering and environmental impacts of Karst, pp 91–102
Li LH, Yang ZF, Yue ZQ, Zhang LQ (2009) Engineering geological characteristics, failure modes and protective measures of Longyou rock caverns of 2000 years old. Tunnel Underground Space Technol 24:190–207
Lollino P, Martimucci V, Parise M (2013) Geological survey and numerical modeling of the potential failure mechanisms of underground caves. Geosyst Eng 16(1):100–112. https://doi.org/10.1080/12269328.2013.780721
Lombardi G, Feola A, Miraglino P (2010) Interventi per la mitigazione del rischio idrogeologico della città di Napoli. Geologi 28:7–17 (**In Italian**)
Mancini F, Stecchi F, Gabbianelli G (2009) GIS-based assessment of risk due to salt mining activities at Tuzla (Bosnia and Herzegovina). Eng Geol 109:170–182
Milia A, Torrente MM, Russo M, Zuppetta A (2003) Tectonics and crustal structure of the Campania continental margin: relationships with volcanism. Mineral Petrol 79(1–2):33–47. https://doi.org/10.1007/s00710-003-0005-5
Morra V, Calcaterra D, Cappelletti P, Colella A, Fedele L, de' Gennaro R, Langella A, Mercurio M, de' Gennaro M (2010) Urban geology: relationships between geological setting and architectural heritage of the Neapolitan area. In: Marco B, Angelo P, Massimo M, Sandro C, Carlo D (eds) The geology of Italy: tectonics and life along plate margins. J Virt Expl Electron Edn. ISSN 1441-8142, vol 36(27). https://doi.org/10.3809/jvirtex.2010.00261
Newton JG (1984) Natural and induced sinkhole development in the eastern United States. In: Proceedings of the third international symposium on land subsidence, international association of hydrological sciences. Wallingford, UK, pp 549–564
Nicotera P, Lucini P (1967) La costituzione geologica del sottosuolo di Napoli nei riguardi dei problemi. Atti dell'VIII Convegno di Geotecnica. Cagliari, pp 45–111 (in Italian)
Nisio S, Caramanna G, Ciotoli G (2007) Sinkholes in Italy: first results on the inventory and analysis. Geol Soc Lond Spec Publ 279(1):23–45. https://doi.org/10.1144/SP279.4
Oh HJ, Lee S (2011) Integration of ground subsidence hazard maps of abandoned coal mines in Samcheok. Korea Int J Coal Geol 86(1):58–72
Orsi G, Di Vito MA, Isaia R (2004) Volcanic hazard assessment at the restless Campi Flegrei caldera. Bull Volcanol 66:514–530. https://doi.org/10.1007/s00445-003-0336-4
Ozdemir A (2015) Investigation of sinkholes spatial distribution using the weights of evidence method and GIS in the vicinity of Karapinar (Konya, Turkey). Geomorphology 245:40–50. https://doi.org/10.1016/j.geomorph.2015.04.034
Ozdemir A (2016) Sinkhole susceptibility mapping using logistic regression in Karapınar (Konya, Turkey). Bull Eng Geol Env 75(2):681–707. https://doi.org/10.1007/s10064-015-0778-x
Parise M (2012) A present risk from past activities: sinkhole occurrence above underground quarries. Carbon Evap 27(2):109–118
Parise M, Lollino P (2011) A preliminary analysis of failure mechanisms in karst and man-made underground caves in Southern Italy. Geomorphology 134(1–2):132–143. https://doi.org/10.1016/j.geomorph.2011.06.008
Parise M, Gunn J (2007) Natural and anthropogenic hazards in karst areas: recognition, analysis and mitigation. Special Publications 279(1). The Geological Society of London, London, UK. ISBN 978-1-86239-224-3. https://doi.org/10.1144/SP279
Parise M, Vennari C (2013) A chronological catalogue of sinkholes in Italy: the first step toward a real evaluation of the sinkhole hazard. In: Land L, Doctor DH, Stephenson B (eds) Proceedings 13th multidisciplinary conference on sinkholes and the engineering and environmental impacts of Karst, Carlsbad

(New Mexico, USA). Natl Cave Karst Res Inst, pp 383–392. https://doi.org/10.5038/9780979542275.1149
Parise M, Galeazzi C, Bixio R, Dixon M (2013) Classification of artificial cavities: a first contribution by the UIS Commission. In: Filippi M, Bosak P (eds) Proceedings 16th international congress of speleology, Brno, 21–28 July 2013, 2, pp 230–235
Parise M (2011) Sinkholes caused by underground quarries in Apulia, southern Italy. In: Proceedings 12th multidisciplinary conference on sinkholes and the engineering and environmental impact of Karst, St. Louis, Missouri, January 10–14, 2011 (Program with Abstracts, 23)
Parise M (2015) A procedure for evaluating the susceptibility to natural and anthropogenic sinkholes. Georisk Assess Manage Risk Eng Syst Geohaz 9(4):272–285. https://doi.org/10.1080/17499518.2015.1045002
Pellicani R, Spilotro G, Gutiérrez F (2017) Susceptibility mapping of instability related to shallow mining cavities in a built-up environment. Eng Geol 217:81–88. https://doi.org/10.1016/j.enggeo.2016.12.011
Pradhan B, Abokharima MH, Jebur MN, Tehrany MS (2014) Subsidence susceptibility mapping at Kinta Valley (Malaysia) using the evidential belief function model in GIS. Nat Hazards 73(2):1019–1042
Rispoli C, Di Martire D, Calcaterra D, Cappelletti P, Graziano SF, Guerriero L (2020) Sinkholes threatening places of worship in the historic center of Naples. J Cult Herit 46:313–319. https://doi.org/10.1016/j.culher.2020.09.009
Rogers CJ (1986) Sewer deterioration studies: the background to the structural assessment procedure in the sewer rehabilitation manual (2nd edn). WRc report ER199E
Scarpati C, Cole P, Perrotta A (1993) The Neapolitan Yellow Tuff—a large volume multiphase eruption from Campi Flegrei, southern Italy. Bull Volcanol 55(5):343–356. https://doi.org/10.1007/BF00301145
Scarpati C, Perrotta A, Lepore S, Calvert A (2013) Eruptive history of Neapolitan volcanoes: constraints from 40Ar-39Ar dating. Geol Mag 150(3):412–425. https://doi.org/10.1017/S0016756812000854
Scotto di Santolo A, Evangelista L, Silvestri F, Cavuoto G, Di Fiore V, Punzo M, Tarallo D, Evangelista A (2015) Investigations on the stability conditions of a tuff cavity: the Cimitero delle Fontanelle in Naples. Rivista Italiana Di Geotecnica XLIX 3:28–46
Scotto di Santolo A, Forte G, De Falco M, Santo A (2016) Sinkhole risk assessment in the metropolitan area of Napoli, Italy. Proc Eng 158:458–463. https://doi.org/10.1016/j.proeng.2016.08.472
Scotto di Santolo A, Forte G, Santo A (2018) Analysis of sinkhole triggering mechanisms in the hinterland of Naples (southern Italy). Eng Geol 237:42–52. https://doi.org/10.1016/j.enggeo.2018.02.014
Shalev E, Lyakhovsky V (2012) Viscoelastic damage modeling of sinkhole formation. J Struct Geol 42:163–170
Sinclair WC, Stewart JW (1985) Sinkhole type, development, and distribution in Florida. Bureau of Geology, Map Series (Tallahassee), vol 110. Florida Department of Natural Resources, Division of Resource Management, Bureau of Geology, Tallahassee, FL, United States. ISSN: 0085-0624
Snyder SW, Evans MW, Hine AC, Compton JS (1989) Seismic expression of solution collapse features from the Florida Platform. In: Multidisciplinary conference on sinkholes and the engineering and environmental impacts of karst, vol 3, pp 281–298
Sottile R (2016) Census and geological study of the anthropogenic sinkholes in the urban area of Palermo (Southern Italy). University of the Study of Siena (PhD thesis).
Subedi P, Subedi K, Thapa B, Subedi P (2019) Sinkhole susceptibility mapping in Marion County, Florida: evaluation and comparison between analytical hierarchy process and logistic regression-based approaches. Sci Rep 9(1):1–18. https://doi.org/10.1038/s41598-019-43705-6
Sunwoo C, Song WK, Ryu DW (2010) A case study of subsidence over an abandoned underground limestone mine. Geosystem Engineering 13(4):147–152. https://doi.org/10.1080/12269328.2010.10541322
Swets JA (1988) Measuring the accuracy of diagnostic systems. Science 240(4857):1285–1293
Taheri K, Gutiérrez F, Mohseni H, Raeisi E, Taheri M (2015) Sinkhole susceptibility mapping using the analytical hierarchy process (AHP) and magnitude–frequency relationships: a case study in Hamadan province. Iran Geomorphol 234:64–79. https://doi.org/10.1016/j.geomorph.2015.01.005
Tharp TM (1999) Mechanics of upward propagation of cover-collapse sinkholes. Eng Geol 52(1–2):23–33
Tharp TM (2002) Poroelastic analysis of cover-collapse sinkhole formation by piezometric surface drawdown. Environ Geol 42(5):447–456
Turco E, Schettino A, Pierantoni PP, Santarelli G (2006) The Pleistocene extension of the Campania Plain in the framework of the southern Tyrrhenian tectonic evolution: morphotectonic analysis, kinematic model and implications for volcanism. Dev Volcanol Elsevier 9:27–51. https://doi.org/10.1016/S1871-644X(06)80016-1

Vitale S, Ciarcia S (2018) Tectono-stratigraphic setting of the Campania region (southern Italy). J Maps 14(2):9–21. https://doi.org/10.1080/17445647.2018.142

Waltham T, Bell F, Culshaw M (2005) Sinkholes and subsidence. Springer, Berlin. https://doi.org/10.1007/b138363

Wilson WL, Beck BF (1992) Hydrogeologic factors affecting new sinkhole development in the Orlando area. Florida Groundwater 30(6):918–930. https://doi.org/10.1111/j.1745-6584.1992.tb01575.x

Yilmaz I (2007) GIS based susceptibility mapping of karst depression in gypsum: a case study from Sivas basin (Turkey). Eng Geol 90(1–2):89–103

Yokota T, Fukatani W, Miyamoto T (2012) The present situation of the road cave in sinkholes caused by sewer systems (FY2006*FY2009). National institute for land and infrastructure management, Ministry of Land, Infrastructure, Transport and Tourism, Japan, Report No. 668 (In Japanese)